RESEARCH PAPERS

Acta Cryst. (1994). B50, 405–414

A Neutron Powder Investigation of the High-Temperature Structure and Phase Transition in $LiNbO_3$

BY H. BOYSEN

Institut für Kristallographie der Universität München, Theresienstrasse 41, D-80333 München, Germany

AND F. ALTORFER

Laboratorium für Neutronenstreuung, ETH Zürich & Paul Scherrer Institut, CH-5232 Villigen PSI, Switzerland

(*Received* 9 *May* 1993; *accepted* 17 *November* 1993)

Abstract

The structure of $LiNbO_3$ has been determined around the phase transition at $T_c \approx 1430$ K by neutron powder diffraction using a mirror furnace in air up to 1505 K. The transition is of the order–disorder type with some displacive components. In the paraelectric high-temperature phase, Li is randomly distributed over two sites on both sides of the O plane and Nb assumes a centrosymmetric position within its O_6 octahedron. There are indications of more complicated disorder and a high mobility of Li. The thermal expansion of the interatomic bonds confirms most of the assumptions given in the classical work of Megaw [*Acta Cryst.* (1968*a*), A**24**, 583–588; *Acta Cryst.* (1968*b*), A**24**, 589–604], in particular, an increase of the tilt angle of NbO_6 octahedra away from the h.c.p. towards the perovskite structure. These octahedra become almost regular at high temperatures. Near T_c there is an abrupt change of Nb—O bonding.

1. Introduction

$LiNbO_3$ has attracted considerable interest over the past few decades, as evidenced by a huge number of publications on this material. This is mainly due to its outstanding physical properties which have led to a wide range of technical applications (for reviews, see *e.g.* Räuber, 1978; Prokhorov & Kuz'minov, 1990). Nevertheless, some important questions still remain open and are subject to some controversy in the literature. Among others, this concerns the character of the phase transition from the low-temperature ferroelectric phase to the high-temperature paraelectric phase at $T_c \approx 1470$ K. In particular, the crystallographic structure of the high-temperature phase has never been determined directly due to experimental difficulties at these high temperatures and its narrow range of existence below the melting point $T_m \approx 1530$ K.

The low-temperature structure with space group $R3c$ has been extensively studied by Abrahams and co-workers (Abrahams, Reddy & Bernstein, 1966; Abrahams, Hamilton & Reddy, 1966; Abrahams, Levinstein & Reddy, 1966; Abrahams & Marsh, 1986). It may be derived from a hexagonal closed-packed array of O atoms with 2/3 of the octahedral interstices filled with cations in the sequence Nb, □, Li, Nb, ... (□ = vacancy) along the threefold axis. Oxygen layers remain planar and equidistant, while the octahedra are slightly distorted and rotated. The high-temperature space group is believed to be $R\bar{3}c$, in agreement with a second-order character of the phase transition. While it is generally agreed that the Nb atoms should move into centrosymetric sites within their octahedra, two models have been proposed for the positions of Li: (i) In the *displacive* model, Li atoms move into triangular coordinated sites within the oxygen layer between the former Li and □ octahedra. (ii) In the *order–disorder* model, the Li atoms are distributed randomly on both sides of this plane.

The disorder model was found from neutron scattering experiments on the isostructural $LiTaO_3$ by Abrahams, Buehler, Hamilton & Laplaca (1973) and is also favoured for $LiNbO_3$ by a number of more recent investigations with different experimental techniques. Chowdhury, Peckham & Saunderson (1978) failed to detect any softening of the ferroelectric mode in their inelastic neutron scattering study. Okamoto, Wang & Scott (1985) in their Raman scattering experiments found a decrease of the peak frequency of that mode, however, they relate this mainly to increasing damping and interpret their spectra (including a quasielastic wing) by a relaxational process with a critical behaviour of the relaxation times as expected for a second-order phase transi-

tion. Further support for the order–disorder model comes from Mössbauer spectroscopy (Tomov, Engelmann, Dézsi & Gonser, 1989) and PAC spectroscopy (Catchen & Spaar, 1991), whereby the latter also found a significant asymmetry of the electric field gradient, *i.e.* a break of the axial symmetry at the Li site. In any case, it should be noted that the disorder model *necessarily* contains some displacive elements too, namely shifts of Nb and O (see below), which are required by the symmetry change $R\bar{3}c \rightarrow R3c$.

Some physical and chemical properties of $LiNbO_3$ differ appreciably with deviations from stoichiometry. A number of corresponding disorder models are proposed in the literature, the most widely accepted being that of Abrahams & Marsh (1986), who from a very careful single-crystal X-ray investigation determined the structure of the so-called congruent composition and found *ca* 5% Nb^{5+} ions at Li sites and corresponding vacancies at Nb sites represented by the formula $[Li_{1-5x}Nb_{5x}][Nb_{1-4x}\square_{4x}]O_3$, with $x = 0.0118$. This model was recently questioned by Iyi *et al.* (1992) who found that Nb sites are always fully occupied and the vacancies are on the Li sites according to the formula $[Li_{1-5x}Nb_x\square_{4x}][Nb]O_3$. Own neutron and X-ray powder investigations on congruent material have recently confirmed this latter model (Zotov, Boysen, Frey, Metzger & Born, 1994).

Abrahams, Levinstein & Reddy (1966) have also performed a high-temperature X-ray powder diffraction study up to 1473 K, but could not obtain a reliable diffraction pattern above T_c due to experimental difficulties. Moreover, their results below T_c suffer from extremely large error bars. In this paper we present the results of neutron powder diffraction experiments in air up to 1505 K using the advantages of neutrons: (1) the bulkier samples reduce the risk of chemical reactions which take place predominantly at the surface of the sample, and (2) the more favourable scattering length of Li allows a more reliable detection of this atom, which plays a key role in the phase transition. Moreover, it was intended to study the high-temperature mobility of Li by also refining anharmonic temperature factors. A very large mobility of Li has been described in some of the aforementioned papers. Ionic conductivity at high temperatures was reported by Jorgensen & Bartlett (1969) and Khachaturyan, Gabrielyan & Kolesnik (1988). The presence of anharmonic thermal motion above about 600 K was deduced from X-ray diffraction studies by Ivanov, Chorney, Mikhal'chenko & Venevtsev (1979) and a single-crystal neutron diffraction study at 1200 K by Rettweiler (1988). The results of the latter study were not fully convincing, however, due to extreme extinction problems.

2. Experimental

The sample material of unknown composition was provided by Th. Berthold of Siemens AG/München. It was prepared from the outer regions of the melt remaining after growing a single crystal from a stoichiometric starting material. Hence, it was originally believed to be close to stoichiometry. This would be in agreement with the refined occupancies, which are, however, subject to some uncertainty related to the correct scattering length of Li (see below). On the other hand, the refined lattice constants (see Table 1, checked also by X-ray diffraction) are very close to the values given by Abrahams & Marsh (1986) for the congruent composition. Possibly there is some variation of the composition in our sample, which may be responsible for some of the difficulties described below (but does not affect the main results) and also could explain an unsuccessful determination of T_c by DTA.

The measurements have been obtained on the instrument DMC (Schefer *et al.*, 1990) of the LNS/PSI Villigen.* This instrument is equipped with a 80° multicounter and was run in the 'high-intensity mode' (no primary collimator) at a wavelength of 1.6988 Å, covering the total angular range $15 \le 2\theta \le 135°$ with a 0.1° step width. The sample was kept in a Pt can (8 mm diameter, 10 mm height) and mounted in an ellipsoidal mirror furnace developed by Lorenz (1988). In this furnace the sample may be heated in air, thereby reducing the risk of oxygen loss at high temperatures. The measuring conditions (*i.e.* Pt container in air) were thus identical to those during crystal growth. With an oscillating radial collimator, the parasitic scattering from the furnace walls (Al) could be completely suppressed. Pt reflexions from the sample holder and the thermocouple (Pt–Pt/Rh 10%) suffered from extreme texture problems and had to be excluded from the fit. Temperature stability was about ± 3 K, while the absolute uncertainty including the gradient was about ± 10 K. The sample absorption [$\sigma_{abs}(Li^{nat}) = 70.5$ barns] was measured to be $\mu r = 0.46$ and the data were corrected for it.

Some recrystallization, *i.e.* the formation of larger yellowish single-crystal grains, occurred at the highest temperature, 1505 K. The corresponding texture problems caused some deviations between observed and calculated intensities. Similar deviations were found in a subsequent measurement at room temperature. In spite of this, the refined parameters agreed within three e.s.d's with those of the first room-temperature measurement. Therefore, all calculated errors for the 1505 K measurement quoted in

* A list of raw neutron powder data has been deposited with the IUCr (Reference SE0126). Copies may be obtained through The Managing Editor, International Union of Crystallography, 5 Abbey Square, Chester CH1 2HU, England.

Table 1. *Refined parameters of displacive model* (I)

	300 K *R3c*	1200 K *R3c*	1350 K *R3c*	1450 K $R\bar{3}c$	1480 K $R\bar{3}c$	1505 K $R\bar{3}c$
z(Li)	0.3021 (9)	0.2885 (17)	0.2850 (10)	$\frac{1}{4}$	$\frac{1}{4}$	$\frac{1}{4}$
z(Nb)	0.0192 (3)	0.0127 (3)	0.0090 (7)	0	0	0
x(O)	0.0478 (4)	0.0573 (6)	0.0564 (11)	0.0591 (4)	0.0602 (6)	0.0598 (18)
y(O)	0.3428 (7)	0.3361 (10)	0.3299 (19)	$\frac{1}{3}$	$\frac{1}{3}$	$\frac{1}{3}$
n(Li)	1.02 (4)	0.85 (3)	0.87 (4)	0.92 (4)	0.91 (6)	1.03 (21)
n(Nb)	1.02 (1)	1.00 (1)	1.02 (1)	1.01 (1)	1.03 (2)	1.00 (6)
β_{11}(Li)	0.014 (6)	0.040 (5)	0.054 (8)	0.043 (7)	0.028 (9)	0.053 (33)
β_{33}(Li)	0.006 (2)	0.014 (3)	0.002 (2)	0.039 (3)	0.033 (5)	0.053 (21)
β_{11}(Nb)	0.003 (2)	0.020 (1)	0.021 (1)	0.021 (1)	0.021 (2)	0.014 (6)
β_{33}(Nb)	0.0003 (–)*	0.0018 (2)	0.0015 (2)	0.0021 (2)	0.0027 (3)	0.0027 (9)
β_{11}(O)	0.001 (2)	0.030 (2)	0.034 (5)	0.029 (1)	0.030 (2)	0.028 (6)
β_{22}(O)	0.002 (1)	0.020 (1)	0.021 (1)	0.027 (1)	0.023 (2)	0.019 (6)
β_{33}(O)	0.0006 (1)	0.0027 (1)	0.0036 (2)	0.0035 (1)	0.0032 (2)	0.0027 (6)
β_{12}(O)	−0.002 (1)	0.012 (2)	0.018 (4)	0.013	0.012	0.009
β_{13}(O)	0.0005 (5)	−0.0035 (7)	−0.0051 (8)	−0.0023 (1)	−0.0023 (2)	−0.0018 (6)
β_{23}(O)	−0.0006 (3)	−0.0034 (2)	−0.0047 (3)	−0.0046	−0.0047	−0.0035
a (Å)	5.1513 (8)	5.2542 (6)	5.2718 (8)	5.2850 (8)	5.2898 (12)	5.2924 (36)
c (Å)	13.8654 (8)	13.8759 (6)	13.8604 (9)	13.8488 (8)	13.8485 (12)	13.8462 (39)
R_{wp} (%)	9.62	6.81	9.37	8.60	12.98	13.17
GOF_{wp}	2.74	2.04	1.33	1.97	1.59	2.69
R_{wI} (%)	4.87	1.68	4.74	4.46	8.63	9.23
GOF_{wI}	6.40	2.34	2.98	4.17	4.25	7.49

* At room temperature Nb was refined isotropically to avoid (non-significant) negative β_{33}.

the tables were arbitrarily enlarged by a factor of three. It should be mentioned that the overdetermination (*ca* 45 reflexions, 16–17 structural parameters for the two standard models) is relatively poor in the present experiment. Nevertheless, we have confidence in the results, since for room temperature they agree well (within two e.s.d.'s) with those obtained from a repeated measurement on the same sample on instrument MAN1 at the FRM/Garching (Hornsteiner, 1993) using a larger sin θ/λ range (225 reflexions), as well as the values given by Abrahams, Reddy & Bernstein (1966), Iyi *et al.* (1992) and Zotov, Boysen, Frey, Metzger & Born (1994). Furthermore, the main intention of the present paper was to distinguish between two alternative models, which can be safely made on the basis of the R factors and the physical significance of the obtained parameters.

3. Data analysis and results

In the high-temperature space group $R\bar{3}c$, atoms are located at

Li (6*a*) 0 0 1/4 $n = 1$ [displacive model (I)]

or Li (12*c*) 0 0 w $n = 1/2$ [disorder model (II)]

Nb (6*b*) 0 0 0

O (18*e*) u 1/3 1/12

plus symmetry-related positions (n = occupancy). The active irreducible representation (IR) leading to the low-temperature space group $R3c$ is Γ^{2-} (A_{2u}). Projection operator techniques give the following critical modes [using the sequence of atoms as given in *International Tables for X-ray Crystallography* (1965, Vol. I)]

$$\varphi_1 = \{(0,0,1),(0,0,1)\}\delta z(\text{Li}) \quad \text{(I)}$$

$$\varphi_1' = \{(0,0,1),(0,0,1),(0,0,1),(0,0,1)\}\delta z(\text{Li}) \quad \text{(II)}$$

$$\varphi_2 = \{(0,0,1),(0,0,1)\}\delta z(\text{Nb})$$

$$\varphi_3 = \{(1,2,0),(-2,-1,0),(1,-1,0),(1,2,0),(-2,-1,0),(1,-1,0)\}\delta y(\text{O})$$

$$\varphi_4 = \{(0,0,1),(0,0,1),(0,0,1),(0,0,1),(0,0,1),(0,0,1)\}\delta z(\text{O}).$$

The order–disorder process of model II is described by

$$\eta = \{1,-1,1,-1\}\delta n(\text{Li}).$$

In addition, there are further degrees of freedom corresponding to the totally symmetric IR Γ^{1+} (A_{1g})

$$\varphi_5 = \{(0,0,1),(0,0,-1),(0,0,1),(0,0,-1)\}w(\text{Li}) \quad \text{[(II) only]}$$

$$\varphi_6 = \{(1,0,0),(0,1,0),(-1,-1,0),(-1,0,0),(0,-1,0),(1,1,0)\}u(\text{O}).$$

In $R3c$, the coordinates are

Li (6*a*) 0 0 z $n = 1$ (I)

or { Li (6*a*) 0 0 z $n = 1/2 + \delta n$; Li′ (6*a*) 0 0 z $n' = 1/2 - \delta n$ } (II)

Nb (6*a*) 0 0 z

O (18*b*) x y z.

Therefore, in terms of the critical parameters we have

$$z(\mathrm{Li}) = 1/4 + \delta z(\mathrm{Li}) \quad \text{(I)}$$

or
$$\left\{ \begin{array}{l} z(\mathrm{Li}) = w(\mathrm{Li}) + \delta z(\mathrm{Li}) \\ z(\mathrm{Li}') = -w(\mathrm{Li}) + \delta z(\mathrm{Li}) \end{array} \right\} \quad \text{(II)}$$

$$z(\mathrm{Nb}) = \delta z(\mathrm{Nb})$$
$$x(\mathrm{O}) = u(\mathrm{O}) + \delta y(\mathrm{O})$$
$$y(\mathrm{O}) = 1/3 + 2\delta y(\mathrm{O})$$
$$z(\mathrm{O}) = 1/12 + \delta z(\mathrm{O}).$$

Since in the polar space group $R3c$ the choice of origin along the z axis is arbitrary, we fix $z(\mathrm{O}) = 1/12$, *i.e.* $\varphi_4 = \delta z(\mathrm{O}) = 0$. This setting was also preferred by Megaw (1968*a*), since it gives directly the Nb displacement from the centre of the octahedron (mode φ_2). φ_1 [model (I)] or φ_1' and φ_5 (II), respectively, describe the displacements of Li, φ_3 a distortion and φ_6 a rotation of the NbO_6 octahedra.

The data were evaluated with the Rietveld program version of Thomas & Bendall (1978), which has been extended for anharmonic temperature factors (Boysen, 1992). Gaussian peak shapes and a manually defined background were used. Neutron scattering lengths were taken from the most recent compilation of Koester, Rauch and Seymann (Sears, 1992): $b_{\mathrm{Li}} = -1.90\ (2)$ fm, $b_{\mathrm{Nb}} = 7.054\ (3)$ fm and $b_{\mathrm{O}} = 5.803\ (4)$ fm. In older compilations the values for Li differ appreciably. In the refinement of congruent $LiNbO_3$ mentioned above, a consistent result could only be achieved using a value close to that quoted by Yelon (1983): $b_{\mathrm{Li}} = -2.03$ fm. Hence, there remains some uncertainty for the final values of the Li occupancies, in particular, a composition not too far from congruent (but again with the Li site vacancy model!) is not implausible. The possibility that our sample was Li^6 depleted could be ruled out by a comparison of the measured and calculated absorption coefficient μ. Examples of observed and calculated powder patterns are shown in Fig. 1.

The results of the refinements for the displacive model I are given in Table 1. In addition to the usual weighted profile agreement indicator $R_{\mathrm{wp}} = [\sum w(y_{\mathrm{obs}} - y_{\mathrm{calc}})^2/\sum w y_{\mathrm{obs}}^2]^{1/2}$ and the corresponding goodness-of-fit $\mathrm{GOF}_{\mathrm{wp}} = R_{\mathrm{wp}}/R_{\mathrm{pexp}} = [\sum w(y_{\mathrm{obs}} - y_{\mathrm{calc}})^2/(m-p)]^{1/2}$ [y are the individual profile intensities, w their weights, m their number and p the *total* (= structural + instrumental) number of refinable parameters], the *weighted R* factor for the integrated intensities $R_{\mathrm{wI}} = [\sum W(I_{\mathrm{obs}} - I_{\mathrm{calc}})^2/\sum W I_{\mathrm{obs}}^2]^{1/2}$ is given. This allows comparison with a statistically expected R_{Iexp}: $\mathrm{GOF}_{\mathrm{wI}} = R_{\mathrm{wI}}/R_{\mathrm{Iexp}} = [\sum W(I_{\mathrm{obs}} - I_{\mathrm{calc}})^2/(M-P)]^{1/2}$, where I are the reflexion intensities, W their weights, M the number of reflexions and P the number of *structural* parameters only. This is preferred for the comparison of different structural models when there are not too many overlapping reflexions (Boysen, 1992). At 1350 K the results are given for Li in the usual Li octahedron (to be consistent with a purely displacive model), although a second (lower) minimum was found for Li in the usually vacant octahedron: $\mathrm{GOF}_{\mathrm{wp}} = 1.30$, $\mathrm{GOF}_{\mathrm{wI}} = 2.74$. All parameters remained essentially the same, except $z(\mathrm{Li}) = 0.2274\ (12)$, $z(\mathrm{Nb}) = 0.0072\ (7)$, $\beta_{33}(\mathrm{Nb}) = 0.0023\ (2)$ and $\beta_{13}(\mathrm{O}) = 0.0001\ (10)$. At 1450 K a slightly better fit could be obtained in space group $R3c$ again with Li in the □ octahedron. Note that the phase transition cannot be detected directly by inspection of the diagram, *e.g.* from the vanishing of specific reflexions. The deviations $\delta z(\mathrm{Nb})$ and $\delta y(\mathrm{O})$ [but not $\delta z(\mathrm{Li})$] were, however, very small (less than two e.s.d.'s), and in the disorder model (below), unphysical results were obtained. We, therefore, only

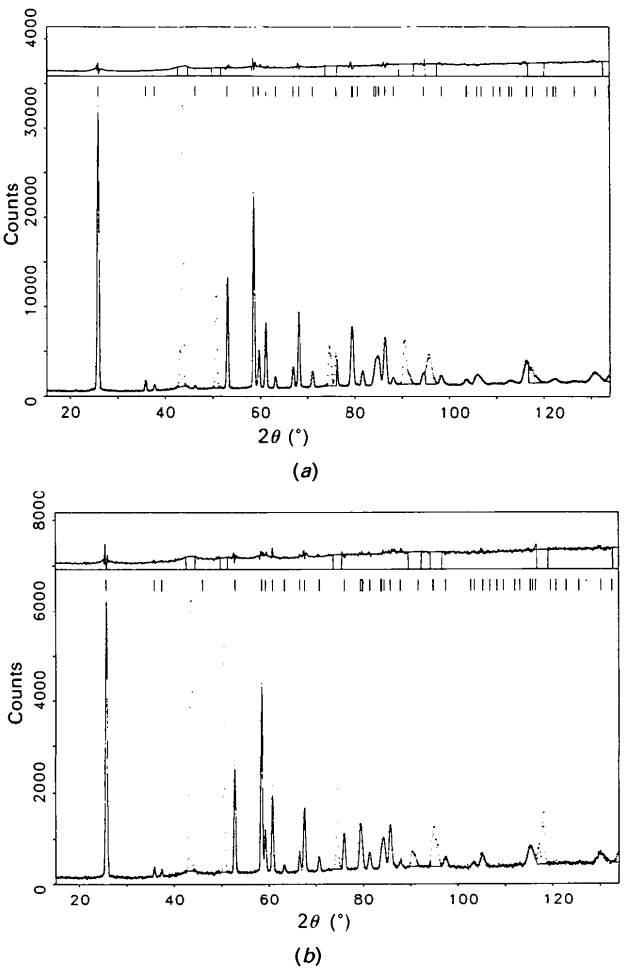

Fig. 1. Observed (dots) and calculated (solid line) powder patterns at (*a*) 1200 and (*b*) 1480 K. Reflexion positions are marked (Pt reflexions excluded from the fit) and the background ($y_{\mathrm{obs}} - y_{\mathrm{calc}}$) is shown on the top.

Table 2. *Refined parameters of disorder model* (II)

	1200 K $R3c$	1350 K $R3c$	1450 K $R\bar{3}c$	1480 K $R\bar{3}c$	1505 K $R\bar{3}c$
z(Li)	0.2875 (17)	0.2762 (13)	0.2813 (8)	0.2812 (10)	0.2905 (39)
z(Nb)	0.0128 (4)	0.0093 (7)	0	0	0
x(O)	0.0576 (6)	0.0569 (9)	0.0595 (3)	0.0607 (5)	0.0597 (15)
y(O)	0.3369 (11)	0.3297 (15)	$\frac{1}{3}$	$\frac{1}{3}$	$\frac{1}{3}$
n(Li)/n(Li′)	0.75 (8)/0.10 (8)	0.33 (7)/0.57 (8)	0.85 (3)	0.85 (5)	1.00 (18)
n(Nb)	1.00 (1)	0.99 (1)	1.01 (1)	1.04 (2)	0.99 (6)
β_{11}(Li)	0.040 (5)	0.070 (9)	0.047 (6)	0.030 (8)	0.059 (33)
β_{33}(Li)	0.012 (4)	0.002 (1)	0.001 (1)	0.002 (2)	0.003 (6)
β_{11}(Nb)	0.020 (1)	0.018 (1)	0.021 (1)	0.020 (2)	0.013 (6)
β_{33}(Nb)	0.0018 (2)	0.0019 (2)	0.0017 (2)	0.0023 (3)	0.0026 (9)
β_{11}(O)	0.028 (2)	0.036 (5)	0.028 (1)	0.028 (2)	0.029 (6)
β_{22}(O)	0.0200 (9)	0.022 (1)	0.026 (1)	0.022 (2)	0.019 (6)
β_{33}(O)	0.0027 (1)	0.0034 (2)	0.0034 (1)	0.0029 (2)	0.0024 (6)
β_{12}(O)	0.011 (2)	0.018 (4)	0.013	0.011	0.010
β_{13}(O)	−0.0030 (8)	−0.0020 (10)	−0.0023 (1)	−0.0024 (2)	−0.0019 (6)
β_{23}(O)	−0.0034 (2)	−0.0047 (3)	−0.0047	−0.0047	−0.0037
a (Å)	5.2542 (6)	5.2719 (8)	5.2849 (8)	5.2897 (12)	5.2923 (36)
c (Å)	13.8759 (6)	13.8601 (8)	13.8481 (8)	13.8476 (12)	13.8451 (36)
R_{wp} (%)	6.81	9.05	8.51	12.66	12.62
GOF_{wp}	2.04	1.29	1.95	1.55	2.58
R_{wI} (%)	1.68	4.20	4.25	7.74	8.61
GOF_{wI}	2.38	2.69	4.03	3.87	7.10

quote the results for $R\bar{3}c$. Possibly this temperature was rather close to T_c. The β_{33}(Li) values are extremely large in the high-temperature phase corresponding to r.m.s. amplitudes of *ca* 0.6 Å along **c**, a very strong hint towards the disorder model. Another hint in favour of model II are the decreased Li occupancies at high temperatures. The results given here for model (I) are not inconsistent with those of Abrahams, Levinstein & Reddy (1966). A real comparison is, however, hampered by the very large errors given by these authors.

The results for model (II) are summarized in Table 2. Here we have constrained $z(\text{Li}') = 1/2 - z(\text{Li})$ in the low-temperature phase, *i.e.* the distance of Li and Li′ (in the □ octahedron) from the neighbouring O-plane is assumed to be the same. A free z(Li′) gave no difference at 1350 K while at 1200 K $z(\text{Li}') \approx 0.25$ was found, however, with no significant improvement of the fit ($GOF_{wI} = 2.41$). At 1200 K the disorder model is not significantly better and essentially the same as model (I): GOF_{wp} is unchanged, GOF_{wI} is slightly worse and n(Li′) almost equal to its e.s.d. At all higher temperatures, however, model (II) provides the better fit. Note that this may be seen more clearly from the GOF_{wI}'s instead of the GOF_{wp}'s, as expected (Boysen, 1992).

The total occupancies of Li are still too low and indicate further disorder. Therefore, a number of test refinements have been carried out using additional split positions (also for Nb and O), as well as anharmonic temperature factors. Some gave considerable improvement of the fits and, very importantly, total Li occupancies in agreement with the room-temperature values. Unfortunately, however, the results were not fully reliable: different models gave similar R factors, some parameters were not physically meaningful and had very large errors. This is of course a consequence of the limited number of reflexions and the rapid increase of parameters in more complex models. Nevertheless, these refinements strongly indicated a more complicated disorder at high temperatures.

4. Discussion

From the evidence given above it is clear that the high-temperature structure and the phase transition are mainly of the order–disorder type. Inspection of Tables 1 and 2 shows that apart from z(Li) and n(Li), all other structural parameters are to a good approximation, independent of the model. Analysis of the anisotropy of (harmonic) thermal motion shows that Nb remains almost isotropic at all temperatures, Li is extended along **c** and O roughly perpendicular to the Nb—O bond. This is illustrated in Fig. 2 for 1200 K. Note that the O ellipsoid cannot be exactly perpendicular to all Nb—O bonds, since the Nb—O—Nb bond angle is less than 180°. The form of these ellipsoids points towards a rotation of almost rigid NbO_6 octahedra (strong Nb—O bonds). At 1350 K there are some striking changes: β_{33}(Li) is strongly reduced, y(O) becomes less than 1/3, and the (majority of) Li's have entered the originally empty octahedron.

The test refinements mentioned above suggested a more complicated disorder at high temperatures. As an illustration (without claiming too much significance to the details), the probability density function (p.d.f.) of Li (and Nb), obtained by Fourier transformation of the refined anharmonic temperature factors [*International Tables for X-ray Crystallography* (1974, Vol. IV), pp. 311–336.], is shown in Fig. 3

for 1200 K. It is considerably spread out, extending partly into the □ octahedron. This rather broad distribution is suggestive of a diffusive motion of the Li's. At higher temperatures (not shown because of some larger unphysical negative regions), two distinct maxima occur on both sides of the O plane. This may be interpreted as increasing (with temperature) jump rates of diffusing Li. Another feature shown in the inset of Fig. 3 is a threefold anisotropy around the *c* axis, *i.e.* a loss of axial symmetry, which has also been reported by Catchen & Spaar (1991).

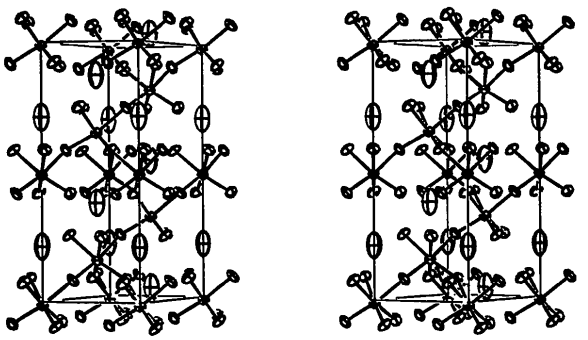

Fig. 2. Stereo-*ORTEP* (Johnson, 1965) plot of $LiNbO_3$ at 1200 K. Thermal ellipsoids correspond to 80% probability. Nb—O bonds are outlined.

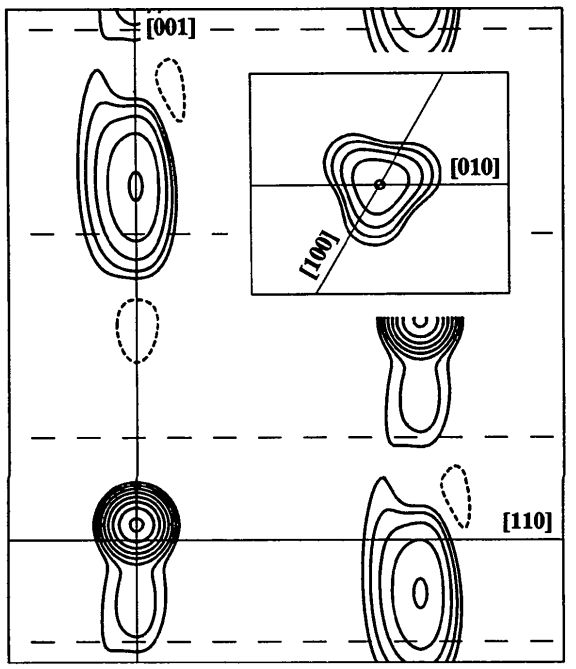

Fig. 3. P.d.f. maps of Li (and Nb, nearly isotropic) at 1200 K, (11.0)-section. Contour lines refer to 6%, 12%, 24%, 48% and 96% of maximum. Small dashed lines indicate negative regions. Long dashed lines (straight) show the positions of the O layers. The inset shows a [001]-section through the Li position.

Fig. 4 shows the temperature dependence of the order parameters Q_i corresponding to the critical modes φ_i, which have been normalized at 25 K [$Q_i = \varphi_i(T)/\varphi_i(25\ \mathrm{K})$]. Here and in the following figures we have included the values of 25 and 70 K obtained by Hornsteiner (1993). Only φ_2 (the off-centre displacement of Nb which mainly determines the polarization) follows an expected critical behaviour. A fit to a critical law $Q_2 = [(T_c - T)/T_c]^\beta$ gave $T_c =$ 1390 (40) K and $\beta = 0.22\ (4)$, *cf.* the solid curve in Fig. 4. Although T_c would again be more consistent with a congruent composition of our sample and β could indicate a tricritical behaviour, these values should not be taken too seriously due to the very small number of data points and possible deviations of the critical law at very low temperatures. Q_3 is below this curve and even negative at 1350 K, however, with large e.s.d.'s. In the displacive model Q_1 lies far above the Q_2-curve, again a very strong indication that the disorder model is in fact the correct one, since for a purely displacive second-order phase transition one would expect all order parameters belonging to the same IR to follow the same temperature dependence. To calculate Q_1' for the disorder model both z(Li) and z(Li′) are needed. Since they could not be obtained unambiguously in the refinement we tentatively assume w (φ_5) to be

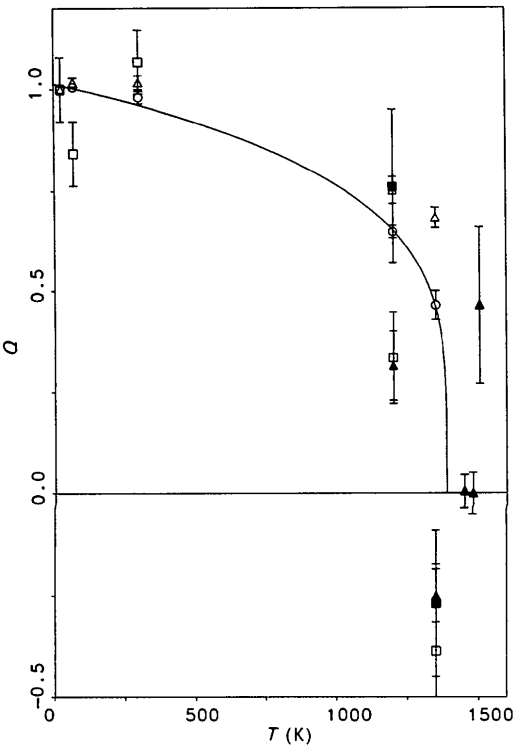

Fig. 4. Temperature dependence of normalized order parameters: Q_1 (△), Q_1' (▲), Q_2 (○), Q_3 (□) and Q_7 (■). The solid line represents the fit of a critical law to Q_2 only.

independent of temperature and equal to the value above T_c (disregarding the value at 1505 K with its large uncertainty). Then the resulting Q'_1 is very close to Q_3, in particular it is also negative at 1350 K. Moreover, Q_η, the order parameter corresponding to the occupation, is negative at 1350 K. This implies a strong correlation between the occupancy and position of Li with the φ_3 distortion of the NbO_6 octahedra. It has to be mentioned that an equivalent alternative view is to keep Q'_1, Q_3 and Q_η positive and Q_2 negative, which would mean to put the anomaly on the Nb displacement. This would, however, correspond to a reversal of the polarization of the ferroelectric domain which seems not to have been observed and also does not lead to a smooth consistent critical behaviour of Q'_1, Q_3 and Q_η. In view of the rather large errors, it cannot be completely ruled out that Q'_1, Q_3 and Q_η are in fact zero already at 1350 K. This would imply a different T_c for these parameters as distinct from that of Q_2, which is clearly non-zero at 1350 K. In any case, it can be concluded that the phase transition is of the order–disorder type with a displacive precursor also for Li. This picture is in agreement with the results of Okamoto, Wang & Scott (1985).

The results obtained here may be compared with the theoretical analysis of the $LiNbO_3$ structure given by Megaw (1968*a*,*b*; see also Megaw, 1973; Megaw & Darlington, 1975). In this treatment, the structure is envisaged as a corner-linked framework of NbO_6 octahedra, thereby emphasizing the much stronger Nb—O bond compared with Li—O. The thermal ellipsoids indicating large rotational motions of these units (see Fig. 2) nicely confirm this view. The thermal expansion is then split into a change of shape and size of the octahedra and a change of tilt relative to one another, the effect of the latter being expected to be much larger than the former. Megaw (1968*a*) further points out the possibility of a continuous change from the h.c.p. to the perovskite structure by such a rotation of the octahedra around the triad axis (mode φ_6). The tilt angle of the NbO_6 octahedron is given by

$$\tan \omega = 3(3)^{1/2}u/(2 - 3u),$$

where $u = 0$ ($\omega = 0°$) corresponds to ideal close packing and $u = 1/6$ ($\omega = 30°$) to ideal perovskite. At room temperature $\omega \approx 6.5°$ in $LiNbO_3$. Assuming in a first-order approximation ($\varphi_3 = 0$) regular octahedra with O—O bond length l, an increase of ω leads to an increase of the lattice constant

$$a = l[\sin \omega + (3)^{1/2} \cos \omega].$$

At the perovskite limit ($\omega = 30°$), the framework is fully extended. The lattice constant

$$c = 2(6)^{1/2}l$$

is of course independent of tilting. Therefore, following Megaw & Darlington (1975), one may define an octahedron strain ζ which describes a flattening or elongation of the octahedra

$$c/a = \{2(6)^{1/2}/[\sin \omega + (3)^{1/2} \cos \omega]\}(1 + \zeta).$$

Naturally one expects an increase of ω (increase of specific volume) with temperature, which was already noticed by Megaw on the basis of the data of Abrahams, Levinstein & Reddy (1966), and is more clearly confirmed here, as shown in Fig. 5. There is no anomaly at T_c, as expected for this non-critical parameter. Note that this tendency is towards the perovskite structure, which has, therefore, to be taken as the aristotype structure. Moreover, in perovskite the octahedra are strictly regular. Fig. 6 shows that the octahedron strain ζ indeed decreases strongly with temperature.

Another effect of the tilting of the NbO_6 octahedra is an opening up of the O triangle between the Li and the □ octahedra. The distance between the midpoint of this triangle and the O increases strongly from 1.94 Å at room temperature to about 2.08 Å at high temperature. This latter value may be compared with the Li—O distance at room temperature 2.07 Å (and even 2.05 Å at 25 K), *i.e.* Li can easily pass through this "bottle neck" from one octahedron to the other.

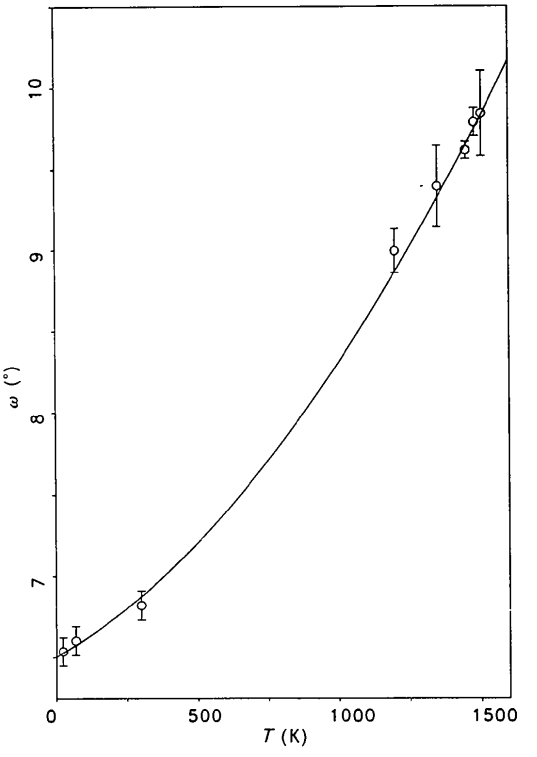

Fig. 5. Temperature dependence of tilt angle ω.

This opening would be wide enough to accommodate Li in the central position as assumed in the displacive model (I). The actual increase of the *average* (smaller) Li—O distance is almost linear up to 2.13 Å at high temperature. In fact, the opening may even be too large for a tight three-coordinated Li—O bond and, therefore, may be responsible for the heavy (probably dynamic) disorder of the Li's suggested above.

Megaw considers the action of the φ_3-mode as a second-order approximation which may be further justified here, since δy(O) is small at all temperatures. With $\delta y(O) > 0$ it leads to an enlargement of the triangle above Nb, a contraction of that below and a rotation of the triangle between Li and □. This means that the off-centre displacement of Nb is towards the larger face at room temperature, while the situation is reversed at 1350 K. Fig. 7 shows the variation of all O—O bond lengths in the NbO_6 octahedron. It clearly illustrates the increasing regularity, which is almost perfect at high temperature. It may be worth mentioning that from the rather uncertain evidence of the data of Abrahams, Levinstein & Reddy (1966), Megaw (1968*b*) derives an increasing difference between the average inclined bonds (dotted line in Fig. 7) and the average of the upper and lower bonds (dashed line) and concludes that the average of all bonds (dash–dotted line) decreases with temperature (which was noted by her as being "certainly anomalous"). From our results, however, both temperature coefficients are of opposite sign and, therefore, much more plausible.

The distortion φ_3 could not be correlated with the Nb displacement φ_2 as might have been expected, but rather with the Li modes φ'_1 (and η), *cf.* Fig. 4. This means that (the majority of) Li is always in the smaller octahedron and thus shows the non-negligible influence of Li—O bonding. On the other hand, φ_2 can be related to the octahedron strain ζ. Such a relation has been suggested by Megaw & Darlington (1975) in analogy with the macroscopic relation between induced spontaneous strain and spontaneous polarization: strain $\propto P_s^2$. This relation may be easily derived from a Landau expansion of the free energy, taking into account the symmetry restrictions imposed to the coupling of order parameters belonging to two different IR's (ζ belongs to Γ^{1+}). P_s can be assumed to be proportional to the Nb displacement δz(Nb) and Fig. 8 nicely confirms this proposition. Note, however, that the straight line does not pass exactly through zero, since the strain does not vanish completely in the high-temperature phase.

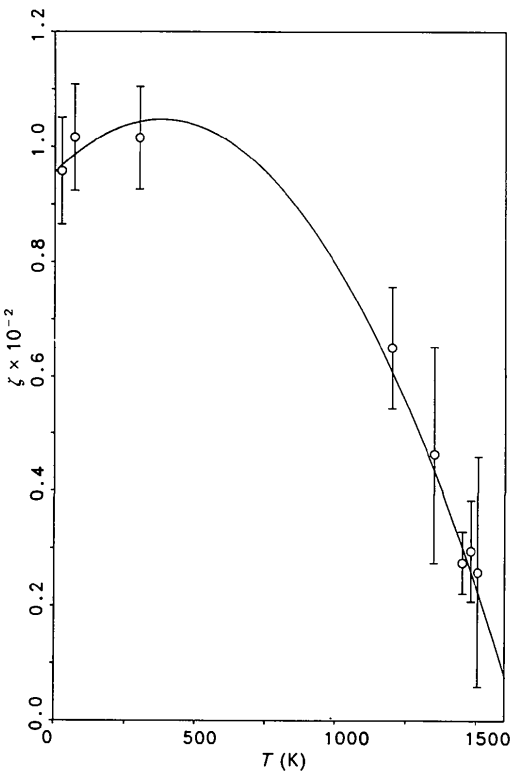

Fig. 6. Temperature dependence of octahedron strain ζ.

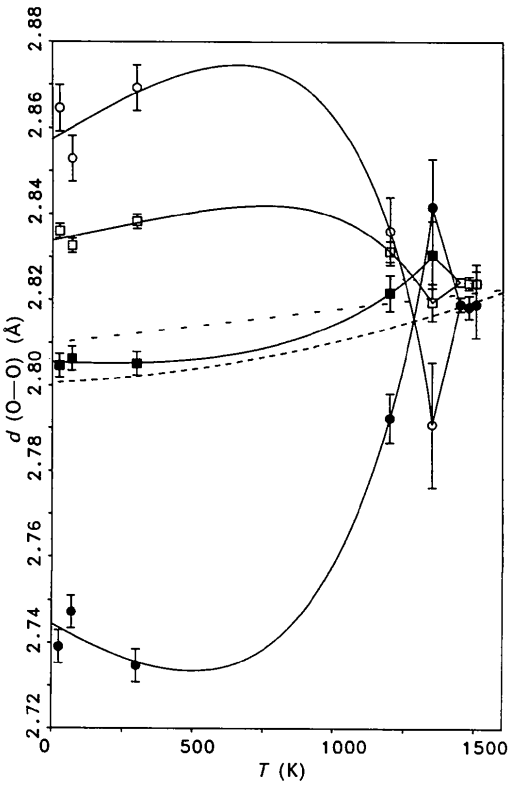

Fig. 7. Temperature dependence of O—O bond length in NbO_6 octahedron: below (●), above (○), inclined 1 (■), inclined 2 (□). Dashed line: average of above and below, dotted line: average of inclined, dash–dotted line: total average.

An interesting feature is observed for the Nb—O distances (Fig. 9), which change almost linearly up to T_c (a consequence of the reversal of φ_3 at 1350 K!) and exhibit a rather abrupt jump near T_c. The average Nb—O distance is almost constant. The Nb—O—Nb bond angle increases from about 138° at room temperature to about 147° at high temperature without any anomaly at T_c, *i.e.* there is also a tendency towards the perovskite value 180°.

The dominant role played by the tightly bonded NbO_6 octahedra as well as the tendency towards the perovskite structure fit well to recent investigations of the local order (Andonov, Chieux & Kimura, 1993) and clustering (Andonov, Kimura & Sawada, 1993) in the melt. Octahedrally coordinated Nb atoms and threefold coordinated Li's have been found up to 100 K above the melting point. With decreasing temperature chains of 3–4 octahedra followed by blocks of $3 \times 2 \times 1$ octahedra (ReO_3-like) and aggregates of $2 \times 2 \times 2$ octahedra (regular, perovskite-like or deformed) appear. There are, however, slight discrepancies between the melt and the solid state for the actual bond lengths. These differences are related to the different short-range structure in the melt and are explained in a forthcoming paper by Andonov, Chieux & Kimura (1994).

In conclusion, the phase transition and thermal changes in $LiNbO_3$ may be visualized as follows. Starting from the idealized fully expanded perovskite arrangement (clusters of which could be present in the melt), upon solidification the framework collapses through tilting of the NbO_6-octahedra around the triad axis. The rather large tilt angle $\Delta\omega \approx 20°$ may be correlated with the small size of the Li cation, as shown by Megaw & Darlington (1975). The two equally sized octahedra not containing Nb are separated by a large enough opening to allow rapid diffusion of Li such that both are occupied with equal probability. Further crumpling (tilting) with decreasing temperature gradually closes this opening, *i.e.* the potential barrier for diffusion becomes larger, leading to an unequal distribution of the Li's below T_c. As a consequence, the faces to the neighbouring Nb octahedra become unequal and the NbO_6 octahedron will be distorted. This in turn allows for an off-centre displacement of the Nb's, because the deviation from regularity becomes appreciable (loss of degeneracy). In the first stage, the stronger (shorter) of the two Nb—O bonds will naturally be associated with a smaller O—O bond length. The reversal observed around 1350 K may then be attributed to the increasing influence of the Nb—Li

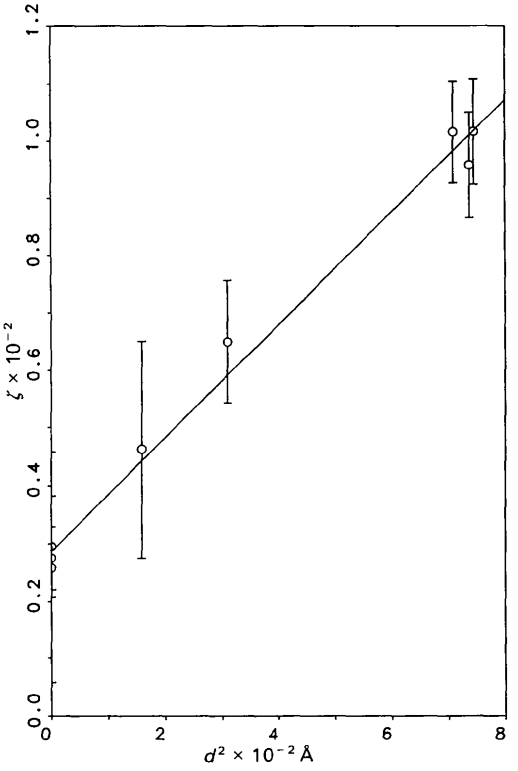

Fig. 8. Relation between octahedron strain ζ and square of Nb displacement $d^2 = [c\delta z]^2$.

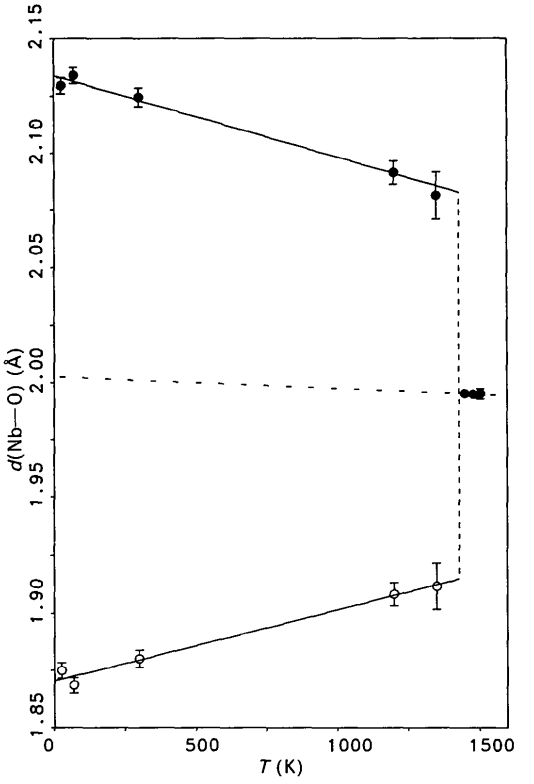

Fig. 9. Temperature dependence of Nb—O (○,●) bond lengths. Dash–dotted line indicates the average of the Nb—O bond lengths.

repulsion, which forces Li into the more distant octahedron such that in adjacent octahedra Li and Nb are located away from their common face.

We are grateful to Dr Th. Berthold (Siemens AG/München) for supplying the sample and Professor W. Eysel (University of Heidelberg) for performing the DTA measurement. Special thanks are due to Dr P. Fischer, who enabled us to carry out the experiment at LNS and helped with stimulating discussions. H.B. also thanks the BMFT for financial support (03SC3LMU).

References

ABRAHAMS, S. C., BUEHLER, E., HAMILTON, W. C. & LAPLACA, S. J. (1973). *J. Phys. Chem. Solids*, **34**, 521–532.
ABRAHAMS, S. C., HAMILTON, W. C. & REDDY, J. M. (1966). *J. Phys. Chem. Solids*, **27**, 1013–1018.
ABRAHAMS, S. C., LEVINSTEIN, H. J. & REDDY, J. M. (1966). *J. Phys. Chem. Solids*, **27**, 1019–1026.
ABRAHAMS, S. C. & MARSH, P. (1986). *Acta Cryst.* B**42**, 61–68.
ABRAHAMS, S. C., REDDY, J. M. & BERNSTEIN, J. L. (1966). *J. Phys. Chem. Solids*, **27**, 997–1012.
ANDONOV, P., CHIEUX, P. & KIMURA, S. (1993). *J. Phys. Condens. Matter*, **5**, 4865–4876.
ANDONOV, P., CHIEUX, P. & KIMURA, S. (1994). *Phys. Scr.*, submitted.
ANDONOV, P., KIMURA, S. & SAWADA, T. (1993). *J. Non-Cryst. Solids*, **156–158**, 783–786.
BOYSEN, H. (1992). In *Accuracy in Powder Diffraction II*, edited by E. PRINCE & J. K. STALICK, pp. 165–174. Washington, DC: NIST Special Publication 846.
CATCHEN, G. L. & SPAAR, D. M. (1991). *Phys. Rev. B*, **44**, 12137–12145.
CHOWDHURY, M. R., PECKHAM, G. E. & SAUNDERSON, D. H. (1978). *J. Phys. C*, **11**, 1671–1683.
HORNSTEINER, A. (1993). Diplomarbeit, Universität München.
IVANOV, S. A., CHORNEY, S. A., MIKHAL'CHENKO, V. P. & VENEVTSEV, YU. N. (1979). *Ukr. Phys. J.* **24**, 662–666.
IYI, N., KITAMURA, K., IZUMI, F., YAMAMOTO, J. K., HAYASHI, T., ASANO, H. & KIMURA, S. (1992). *J. Solid State Chem.* **101**, 340–352.
JOHNSON, C. K. (1965). *ORTEP*. Report ORNL-3794. Oak Ridge National Laboratory, Tennessee, USA.
JORGENSEN, P. J. & BARTLETT, R. W. (1969). *J. Phys. Chem. Solids*, **30**, 2639–2648.
KHACHATURYAN, O. A., GABRIELYAN, A. I. & KOLESNIK, S. P. (1988). *Sov. Phys. Solid State*, **30**, 514–515.
LORENZ, G. (1988). Dissertation, Universität München.
MEGAW, H. D. (1968*a*). *Acta Cryst.* A**24**, 583–588.
MEGAW, H. D. (1968*b*). *Acta Cryst.* A**24**, 589–604.
MEGAW, H. D. (1973). *Crystal Structures: A Working Approach*. Philadelphia: Saunders.
MEGAW, H. D. & DARLINGTON, C. N. W. (1975). *Acta Cryst.* A**31**, 161–173.
OKAMOTO, Y., WANG, P.-C. & SCOTT, J. F. (1985). *Phys. Rev. B*, **32**, 6787–6792.
PROKHOROV, A. M. & KUZ'MINOV, YU. S. (1990). *Physics and Chemistry of Crystalline Lithium Niobate*. New York: Adam Hilger.
RÄUBER, A. (1978). In *Current Topics in Materials Science*, edited by E. KALDIS, Vol. 1, p. 481. Amsterdam: North-Holland.
RETTWEILER, S. (1988). Diplomarbeit, Universität München.
SCHEFER, J., FISCHER, P., HEER, H., ISACON, A., KOCH, M. & THUT, R. (1990). *Nucl. Instr. Methods*, A**288**, 477–485.
SEARS, V. F. (1992). *Neutron News*, **3**(3), 26–37.
THOMAS, M. W. & BENDALL, P. J. (1978). *Acta Cryst.* A**34**, S351.
TOMOV, T., ENGELMANN, H., DÉZSI, I. & GONSER, U. (1989). *Solid State Commun.* **69**, 41–44.
YELON, B. (1983). *Neutron Diffraction Newsletter*.
ZOTOV, N., BOYSEN, H., FREY, F., METZGER, T. & BORN, E. (1994). *J. Phys. Chem. Solids*, **55**, 145–152.

Acta Cryst. (1994). B**50**, 414–425

Method of Crystal-Structure Similarity Searching

BY A. V. DZYABCHENKO

Karpov Institute of Physical Chemistry, ul.Obukha 10, *Moscow* 103064, *Russia*

(*Received* 8 *July* 1993; *accepted* 2 *December* 1993)

Abstract

An algorithm is presented which is used to recognize the similarity of crystal structures by matching a description of one structure against the equivalent descriptions of a second. Equivalent descriptions are considered since there are multiple possible ways of choosing the crystal axes and their origin, the asymmetric unit and atom numbering. Another idea used in the algorithm is to use positional and rotational parameters of the molecular fragments to describe the principal crystal structure. The two structures are considered to be similar if in such descriptions the corresponding cell parameters and the parameters of corresponding fragments differ from each other within the limits specified. As a result of such similarity searching, the type of structural similarity, including the transformation matrix of crystallographic axes and the atom correspondences, is determined. The algorithm has been put to practical use in the *CRYCOM* program. This program is compatible with the Cambridge Structural Database (CSD) through interaction with the *GEOM*78 program of CSD. The latter program is also used in

ISSN 0108-7681